Brief communication

Immune infiltration correlates with transcriptomic subtypes in primary estrogen receptor positive invasive lobular breast cancer

Check for updates

Fangyuan Chen [1], Sayali Onkar[2,3], Jian Zou[4], Yujia Li[4], Haley Arbore[3,5], Sai Maley[6], George Tseng [4], Peter C. Lucas[3,6,7,8], Tullia C. Bruno[2,3], Dario A. A. Vignali[2], Julia Foldi [3], Marija Balic[3], Adrian V. Lee [1,9] ✉ & Steffi Oesterreich[1,8,10] ✉

Understanding interplay of breast cancer and microenvironment is critical. Here we identified two transcriptomic subtypes and five immune infiltration patterns from RNA-seq and multiplex immunohistochemistry from 21 ER + /HER2- ILCs. We found proliferative subtype associated with increased suppressive immune infiltration, and defined a signature associated with lower proliferative, pro-inflammatory TAM infiltration, and improved survival in ER+ breast cancer. Our work identified genes related to ILC immune microenvironment and prognosis.

Immunotherapy (IO) is becoming an important option in breast cancer treatment. In triple-negative breast cancer (TNBC), pembrolizumab showed potential benefits in high-risk early-stage disease and metastases[1,2]. In estrogen receptor-positive, HER2-negative (ER + /HER2-) early-stage breast cancer, tumors with lower ER and higher PD-1 were more likely to respond to neoadjuvant immune checkpoint inhibitors (ICI)[3,4]. However, most trials excluded invasive lobular breast cancer, and the investigation of clinical biomarkers beyond ER, PD-1, or TILs is limited.

Transcriptomic data is useful to identify prognostic biomarkers, including tumor subtypes and immune patterns. The intrinsic molecular subtype was one of the first classification systems derived from patient tumor RNA expression[5]. In TCGA, three ILC subtypes were revealed from tumor RNA-seq data by unsupervised clustering, where the reactive-like subtype had better disease free survival and overall survival than the proliferative subtype[6]. Similar classifications were also derived in the RATHER study[7]. More recently, HR + / HER2- breast cancer was defined further into four subtypes—canonical luminal, immunogenic, proliferation subtypes, and receptor tyrosine kinase (RTK)-driven subtypes, in which RTK-driven subtype

showed worst prognosis[8]. For patterns of immune infiltrate, quantification data is scarce, yet high spatial immune scores have been shown to be related to poor outcome in ER+ breast cancer[9]. While tumor cellularity is by definition negatively correlated with stromal infiltration, and thus often low immune infiltration, like other ER+ breast cancers, ILC exhibit low tumor cellularity but also low T-cell infiltration. Less is known about macrophages, but analysis of TCGA and METABRIC data using M1-like (188 genes) and M2-like signatures (159 genes), curated from transcriptomic data of 1822 samples across 64 cell subtypes[10], showed that tumors with higher M1-like signature or M1/M2 ratio were likely more aggressive with poorer survival[11]. However, the prognostic impact of immune infiltration patterns remain ambiguous, considering decreased estimation accuracy for more complex immune cell subtype composition. Specifically, compared to NSTs, ILC exhibit fewer immune-rich neighborhoods, higher proportions of TIGIT+ CD8+ and PD-1+ T cells, a higher M2:M1 macrophage ratio, and different associations between immune infiltration and disease-free survival[11]. However, most studies excluded ILCs, which had distinct immune infiltration compared

[1]Department of Pharmacology and Chemical Biology, University of Pittsburgh School of Medicine, Pittsburgh, PA, USA. [2]Department of Immunology, University of Pittsburgh School of Medicine, Pittsburgh, PA, USA. [3]UPMC Hillman Cancer Center, Pittsburgh, PA, USA. [4]Department of Biostatistics, University of Pittsburgh, Pittsburgh, PA, USA. [5]Interdisciplinary Biomedical Graduate Program, University of Pittsburgh School of Medicine, Pittsburgh, PA, USA. [6]National Surgical Adjuvant Breast and Bowel Project, Pittsburgh, PA, USA. [7]Department of Pathology, University of Pittsburgh, Pittsburgh, PA, USA. [8]Cancer Biology Program, UPMC Hillman Cancer Center, University of Pittsburgh, Pittsburgh, PA, USA. [9]Institute for Precision Medicine, University of Pittsburgh, Pittsburgh, PA, USA. [10]Women's Cancer Research Center, UPMC Hillman Cancer Center, Magee Womens Research Institute, University of Pittsburgh, Pittsburgh, PA, USA. ✉e-mail: leeav@upmc.edu; oesterreichs@upmc.edu

THE HORMEL INSTITUTE
UNIVERSITY OF MINNESOTA

to no special type (NST) tumors[12,13], thus introducing bias especially in data-driven conclusions. Further research is thus warranted to identify prognostic immune infiltration patterns in ILC tumors specifically.

In this study, we performed integrative analysis of both RNA-seq and multispectral immunohistochemistry (mIHC) data in primary ER + / HER2- ILC. We identified two transcriptomic ILC subtypes, five immune infiltration patterns, and linked the ILC subtypes with immune infiltration. We then correlated gene expression with immune cell density, and defined a tumor associated macrophage (TAM)-Low signature, which was negatively associated with TAM infiltration. We further showed in public datasets that TAM-Low was inversely correlated with presence of proliferating TAMs from GSVA signature score, and predicted improved survival outcomes in ER+ breast cancer.

21 primary ER+ treatment-naive lobular breast tumors were included in our cohort (Supplementary Table 1). We performed RNA-seq in all samples, and mIHC in 13 of the tumors using the same FFPE block (Fig. 1A) (Created with BioRender.com.). We identified *CDH1* truncating mutations in 10 samples from RNA-seq (Supplementary Table 2, Supplementary Fig. 1A). We then computed transcriptomic subtypes using the previously reported TCGA ILC classifier, which used expression of 60 genes to derive three ILC subtypes—immune-related, reactive-like, and proliferative[6]. With this method, we identified 12 proliferative, three reactive-like, and six immune-related tumors in our cohort. We combined the latter two groups as the non-proliferative subtype due to transcriptomic similarities in hierarchical clustering and relatively low sample numbers (Fig. 1B). Consistently, we found higher expression of cell-cycle pathways in the proliferative group, and higher expression of immune-related pathways in the non-proliferative subtype, using reference pathways from the RATHER ILC cohort (enriched pathways of hormone-related and immune-related subtypes, respectively) (Fig. 1C). Specifically, the non-proliferative subtype had higher stromal score and mostly consisted of luminal A and normal-like subtypes. In contrast, the proliferative subtype had higher tumor cell purity, lower stromal composition, and was composed of multiple PAM50 types, including luminal A, luminal B, basal, and HER2-enriched subtypes (Fig. 1D, E). Normal-like and basal subtypes had lower median purity than other subtypes from computation, but all were above 50% (Fig. 1F).

Next, we examined immune infiltration patterns by IHC and mIHC (Fig. 2A). From hematoxylin and eosin staining, TIL infiltration was below 10% in general following the International TILs Working Group protocol, consistent with low infiltration pattern in ER + /HER- primary ILC tumors compared to other subtypes (Supplementary Table 5)[14,15]. For mIHC, 3 to 13 ROIs were selected for each case, and each ROI consisted of one tumor region and one stromal region, where immune cells were counted (Supplementary Tables 1 and 4). In general, macrophage showed highest infiltration, followed by CD4 T cells and CD8 T cells, all with higher infiltration in stromal than tumor regions (Fig. 2B). We analyzed correlations based upon infiltration density of the different immune cells, reflecting their associations within or between tumor and stroma, and we observed three clusters—stromal and tumor B cells, Treg cells and macrophages, and CD4 T cells and CD8 T cells (Fig. 2C). Similar analysis in ER + , HER2 non-negative, ILC primary tumors (n = 109) from TCGA using xCell signature scores[10] also showed macrophages clustered with Tregs within the two major clusters (Supplementary Fig. 1C). Furthermore, we identified five immune infiltration patterns in both stromal and tumor regions from non-negative matrix factorization (NMF) clustering (Fig. 2D). In stromal regions, pattern 1, 3, and 5 had generally low infiltration of all immune cells, pattern 2 had higher macrophages and Tregs, and pattern 4 had higher infiltration of CD4 T cells and CD8 T cells (Fig. 2E, F). Similar immune infiltrating patterns were observed in tumor regions (Supplementary Fig. 1D, E). This suggested a potential immunosuppressive microenvironment in pattern 2 while more immune active environment in pattern 4. Specifically, within each patient, the tumors had up to 5 immune patterns, and were often dominated by 1 (blue arrows) or 2 (orange arrows) co-existing patterns (Supplementary Fig. 1B, F).

We then linked immune infiltration with the ILC transcriptomic subtypes, defined in the previous section. Immune patterns and ILC subtypes are not independent (Chi-squared test $p < 0.01$). The proliferative subtype showed higher infiltration of almost all immune cell types at both stromal and tumor areas than the non-proliferative subtype (Fig. 2G, H). Specifically, pattern 2 (likely immunosuppressive) predominated in the proliferative subtype (Fig. 2I). Altogether, it suggested higher immune infiltration, and potentially more immunosuppressive cell types in the proliferative than non-proliferative ILCs.

Access to both mIHC as well as mRNA expression data allowed us to analyze correlations between gene expression and immune cell infiltration. We therefore calculated Spearman's correlation between expression of each individual gene (26,485 genes, $\log_2$(TPM)) and infiltration of major immune cell type (5 types) in stromal or tumor regions (median number per mm^2 among ROIs), including all possible pairwise combinations. Filtering by FDR < 0.05, we identified 651 significant correlations between expression of genes and immune cell subtypes, all with Spearman's rank correlation coefficient of 0.86 or higher, suggesting strong correlation (Fig. 3A, Supplementary Fig. 2A). The majority of correlations were negative associations between gene expression and macrophage infiltration. Combining genes inversely related with presence of stromal or tumor macrophages, we generated a 'TAM-Low' signature of 483 genes (Fig. 3A, Supplementary Fig. 2B), which was enriched in extracellular matrix pathways (Fig. 3B).

Next we compared signature expression of TAM-Low with marker genes of multiple subtypes of tumor-associated macrophages (Supplementary Table 3) from literature in ER+ primary breast cancer, using RNA-seq of METABRIC and SCAN-B[16–18]. In both datasets, the TAM-Low signature was negatively correlated with proliferating TAMs (Prolif-TAMs) (Fig. 3C), a pro-inflammatory subtype characterized by high expression of HMGB1 and cell cycle-related genes (CCNA2, CDC45, CDK1, MKI67, RRM2, STMN1, TOP2A, and TYMS). In summary, we identified a negative association between the TAM-low signature and tumor associated macrophages, and specifically our data suggested that TAM-low genes such as those from the extracellular matrix (ECM) pathway might hinder the infiltration of proliferating, pro-inflammatory tumor associated macrophages.

And finally, we investigated association of TAM-Low with both survival and therapy response. In ER+ breast cancer, the TAM-Low signature predicted improved relapse free survival as well as overall survival in METABRIC ER+ tumors, adjusting for multiple demographic and clinical variables in multivariate Cox regression (Fig. 3D, E). Result in SCAN-B ER+ tumors was similar but lacked significance (Supplementary Fig. 2D). Kaplan-Meier curves showed TAM-Low as protective factor for survival in both datasets (Supplementary Fig. 2E–G). For therapy response, we analyzed the TAM-Low signature levels in ER + /HER2- primary breast tumors from patients treated with neoadjuvant aromatase inhibitor (AI) in the POETIC trial[19]. Tumors from AI responders and non-responders did not have significant difference in TAM-Low signature expression (Fig. 3F–H). However, we observed significantly lower proliferating TAMs (Prolif-TAM) after AI treatment in the responders, as in line with our prior observation of a negative association between the TAM-Low signature and marker genes of proliferating TAMs (Prolif-TAMs). Using expression of marker genes of other TAM subtypes[18], we failed to identify another set of TAMs significantly different between non-responders and responders, except for lower interferon-primed TAMs (IFN-TAM) at baseline in responders (Fig. 3F). In summary, this data suggests that the TAM-low signature is associated with improved endocrine therapy response and outcome ER+ breast cancer.

Finding biomarkers is essential to guide precision immune therapy in breast cancer. In TNBC, higher tumor-infiltrating lymphocytes and mutation burden predicted higher ICI response rate[20]. In early HR + /HER2- cancer, which had relatively lower mutation incidence and immune infiltration, positive lymph node, ER% < 10%, and combined positive score ≥1 were associated with higher pCR rate with neoadjuvant pembrolizumab treatment[3], and elevated PD-L1 scores, ER% < 50%, PR% < 10%, and
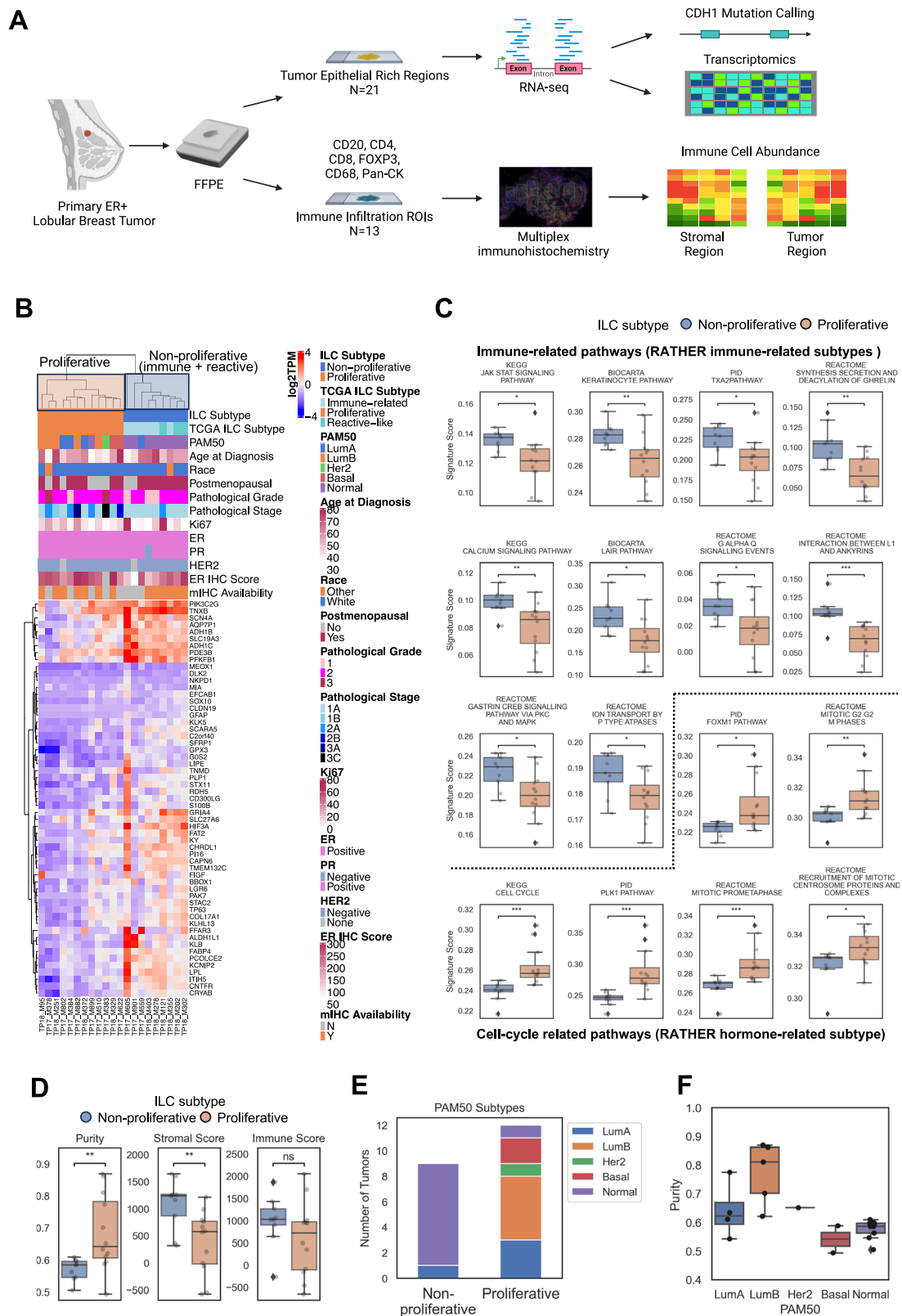
Fig. 1 | Study design and ILC subtype identification from RNA-seq. A Study design and workflow. Treatment-naive ER + /HER2- primary ILC tumors were processed as FFPE blocks, from which FFPE sections underwent RNA-seq in tumor-rich regions selected by pathologist (*N* = 21), and multispectral IHC (mIHC) with immunophenotyping panel (*N* = 13). For mIHC, immune cell infiltration was quantified in regions of interest (ROIs) in both tumor and stromal area. **B** Expression of ILC classifier genes in the ER + /HER2- ILC cohort, showing the two ILC subtypes (proliferative in orange box, non-proliferative (immune + reactive) in blue box), TCGA ILC subtypes, PAM50 subtypes, and other demographic and clinical information. **C** Signature score (ssGSEA score) of reference ILC subtype pathways from RATHER study. Only pathways with significant signature score difference between non-proliferative and proliferative ILC subtypes were shown (Mann-Whitney-Wilcoxon test). **D** Estimated tumor purity, stromal score, and immune score from PUREE and ESTIMATE algorithm. **E** PAM50 subtype composition of non-proliferative and proliferative ILC tumors. **F** Estimated tumor purity in each PAM50 subtype.
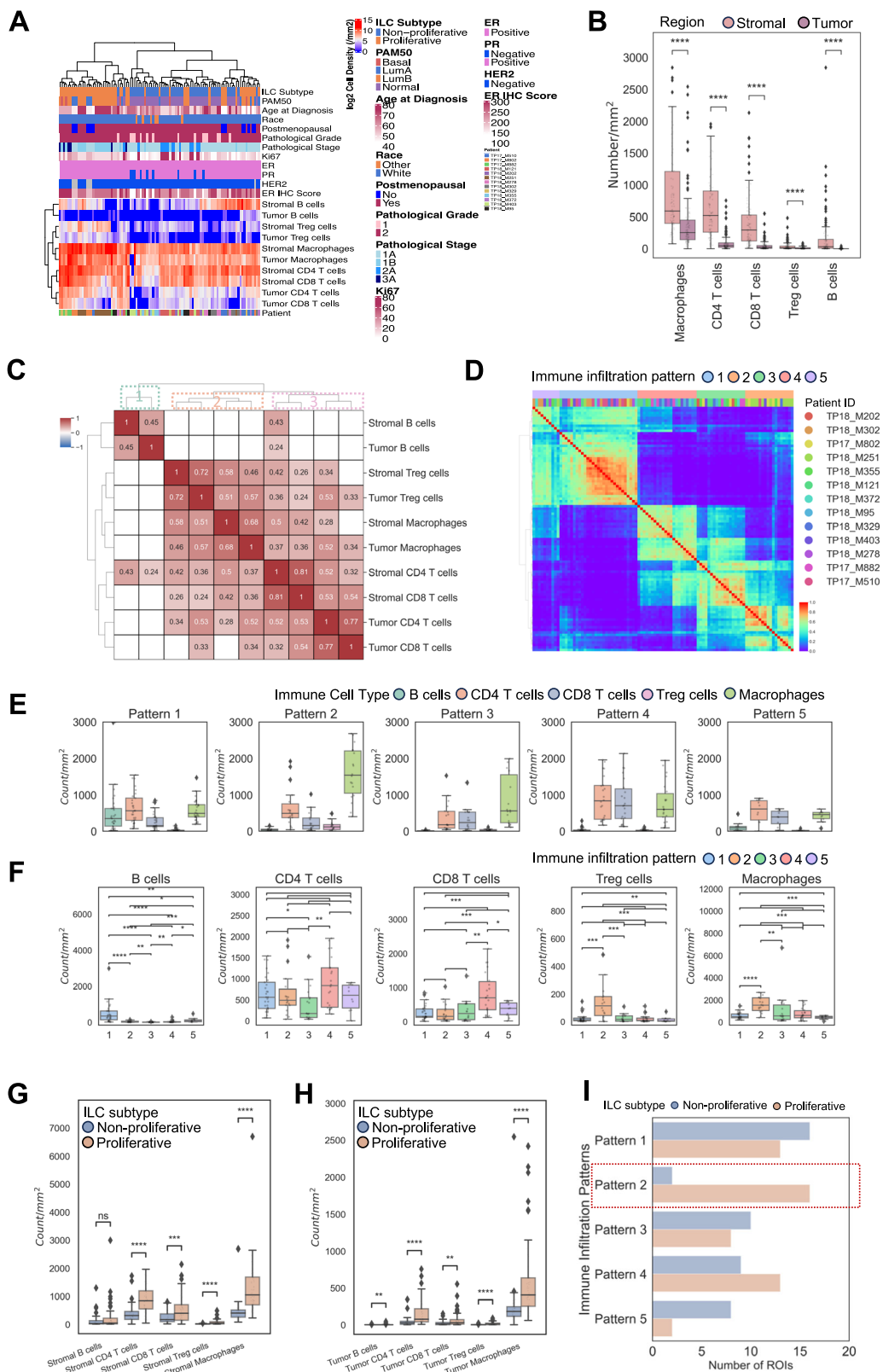
Fig. 2 | **Immune cell infiltration landscape from mIHC. A** Immune cell infiltration in tumor and stromal regions among ROIs ($\log_2$(number/mm^2)), annotated with ILC cluster, PAM50 subtypes, and demographic or clinical information. **B** Histogram of immune cell type abundance (number/mm^2) in stromal and tumor region ROIs. **C** Spearman correlation (FDR < 0.05) of immune cell infiltration (number/mm^2) between cell types. **D** NMF consensus matrix from immune cell infiltration in both stromal and tumor regions among ROIs, showing 5 immune infiltration patterns. **E** Stromal region immune cell infiltration (number/mm^2) among immune infiltration patterns, showing each pattern per panel. **F** Stromal region immune cell infiltration (number/mm^2) among immune infiltration patterns, showing each immune cell type per panel. ****$p < 0.0001$, ***$p < 0.001$, **$p < 0.01$, *$p < 0.05$, comparison (horizontal brackets) with no label, $p \geq 0.05$. **G, H** Immune cell infiltration (number/mm^2) in proliferative and non-proliferative ILC tumors in stromal (**G**) and tumor regions (**H**). **I** Number of ROIs in each immune infiltration pattern, stratified by ILC subtypes.
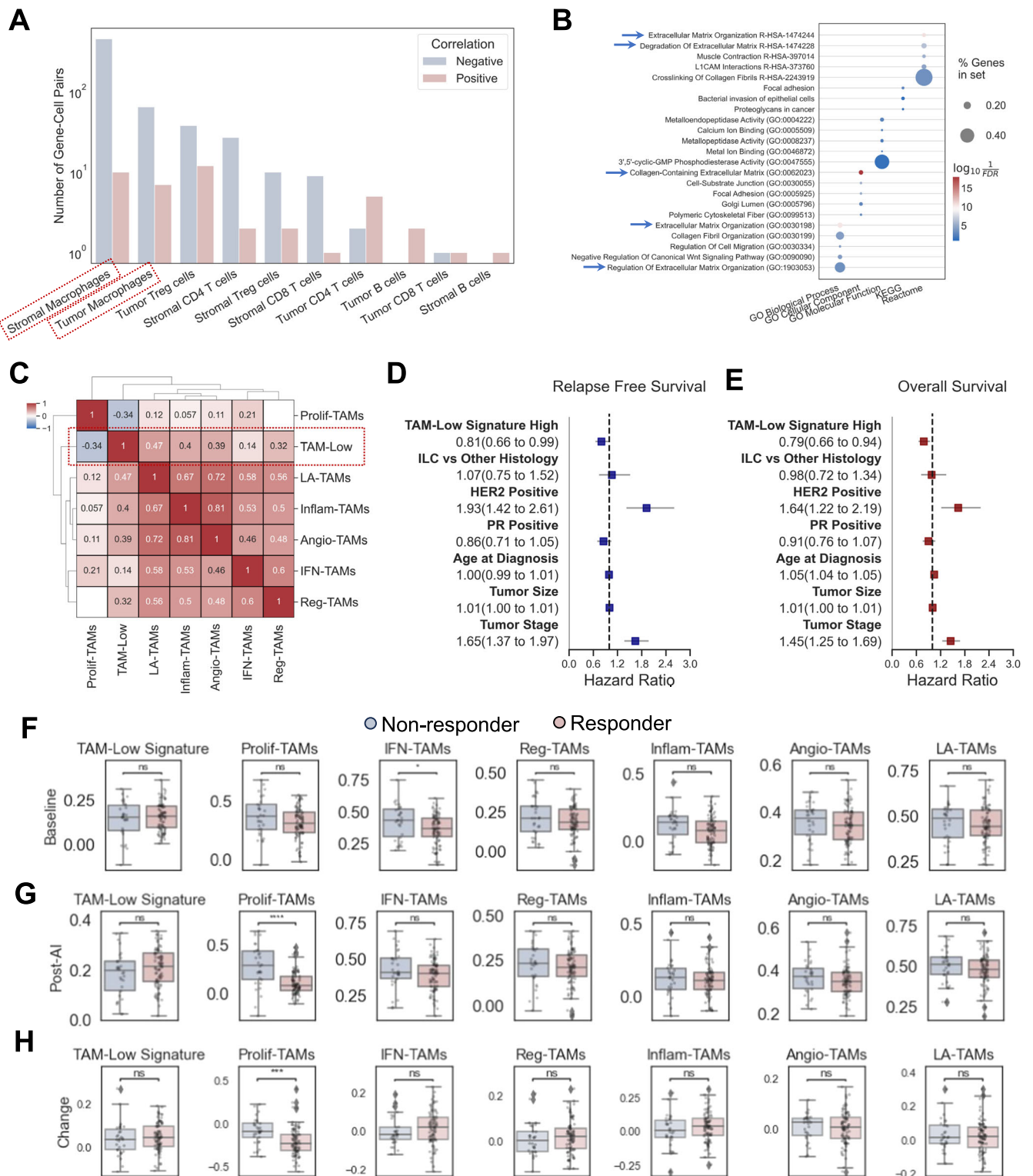
Fig. 3 | Derivation and clinical associations of TAM-Low signature. A Number of gene-cell pairs with significant (FDR < 0.05) positive or negative Spearman's correlation between gene expression (TPM) and immune cell infiltration (median value among ROIs in number/mm²). **B** Pathway enrichment of TAM-Low signature genes (483 genes). **C** Spearman correlation (FDR < 0.05) between TAM-Low and other TAM subtype signatures in METABRIC ER+ tumors (N = 1,505). **D, E** Hazard ratio of relapse free survival (**D**) and overall survival (**E**) of TMA-Neg signature (deconvolution score) and demographic-clinical variables in METABRIC ER+ tumors (N = 1,096, excluding entries with missing data in any of the regression covariates) from multivariant Cox regression. F-H. Deconvolution score of TAM-Low signature and TAM subtype signatures in baseline (**F**), post-aromatase-inhibitor (AI) treatment tumors (**G**), and change after treatment (Δ(Post-AI – baseline)) (**H**) from POETIC trial cohort of 131 patients. IFN-TAMs, interferon-primed TAMs; Reg-TAMs, immune regulatory TAMs, Inflam-TAMs, inflammatory cytokine-enriched TAMs; Angio-TAMs, proangiogenic TAMs; LA-TAMs, lipid-associated TAMs; Prolif-TAMs, proliferating TAMs.

stromal TILs ≥1% indicated pCR and no residual cancer burden with neoadjuvant nivolumab therapy[4]. However, clinical associations of other immune cell types or genes were understudied, and whether pCR translates to long-term survival benefit remained unclear. Moreover, clinical trials did not focus on lobular breast cancer, which had a somewhat distinct immune landscape than NSTs[12,14,21].

Our study focused on primary ER + /HER2- early-stage ILC, and found ILC transcriptomic subtypes were closely related with immune infiltration phenotypes. Specifically, in the proliferative ILC subtype greater infiltration of multiple immune cell types, higher occurrence of immuno-suppressive patterns was also observed. This was consistent with clinical observations that high TIL level in ILC was associated with young age, proliferative tumors, and lymph node invasion[14]. From our previous study, higher macrophage infiltration was related to lower recurrence rate in NST, but this was not observed in ILC[12]. In general, large-scale data is lacking for clinical outcome associations with TIL subtypes or other immune cell types. This hence warrants future effort to incorporate mIHC quantification in prospective cohorts, and to include ILC cases in clinical trials[21].

Most current immunotherapies focus on lymphocytes. However, macrophages, rather than T cells, were dominant in ILCs[12]. In our study, we also found macrophage infiltration as the 'hub' in association with tumor gene expression. Our TAM-Low signature which was directly derived from correlation analysis between gene expression and immune infiltration based on mIHC has potential as a promising biomarker, predicting low infiltration of proinflammatory Prolif-TAMs, and improved survival in patients with ER+ breast cancer. For genes in the TAM-Low signature, extracellular matrix pathways were robustly identified from different databases. For example, *LAMA4*, *LAMB1*, *LAMA2*, and *TNXB* overlap among the top-FDR ranked pathways from Gene Oncology Cellular Component (Collagen-Containing Extracellular Matrix), KEGG (Focal adhesion), and Reactome (Extracellular Matrix Organization). Specifically, *LAMA4*, *LAMB1*, and *LAMA2* encode laminin, constituting key structures of basement membrane; and *TNXB* encodes Tenascin-X, which promotes matrix maturation[22]. Overexpression of these genes thus likely lead to biomechanical rigidity of ECM, which inhibits macrophage infiltration. Interestingly, laminin-targeting therapies improved immune infiltration and drug delivery, and inhibit tumor growth in xenograft mouse models[23]. On the other hand, higher Prolif-TAMs likely marks intrinsic aromatase inhibitor resistance in ER + /HER2- primary breast tumors. As resident tumor macrophages expressing MKI67, CDK1, and CDC45, HMGB1, and others, Prolif-TAMs were likely pro-inflammatory, profibrotic, and promoting tumor progression[18]. In pancreatic ductal adenocarcinoma, targeting Prolif-TAM promoted anti-tumor response via cytotoxic CD8 + T cell redistribution[24]. Interestingly, from our original NST and ILC cohort, we had reported a subgroup of cycling monocytes/macrophages expressing MKI67 and SPP1 genes, which likely corresponded to Prolif-TAMs[12]. Of note, each TAM subtype affects breast cancer differently. For example, the FOLR2+ tumor-stroma-resident macrophages correlated to higher T cell infiltration and better prognosis[25]. Conversely, TREM2+ macrophages likely determined an immunosuppressive metastatic niche, with TREM2 predicting poorer overall survival and relapse-free survival in triple-negative breast cancer[26,27]. Therefore, we encourage quantification of individual TAM subtypes in breast cancer and specifically in ILC as a more accurate immune pheno-typing in clinical response prediction.

Limitations of this study include small cohort size, variations in ROI selection, and absence of immunophenotyping panel of a broader range of immune subtypes, including the macrophage population. There are also limitations to combining different methodologies for analysis of immune cell infiltration and activities, as reflected by some discrepancy between mIHC and RNA-seq deconvolution algorithms—e.g., proliferative ILCs had higher stromal or immune scores and showed lower expression of immune signaling than non-proliferative ones, including the JAK-STAT pathway and local acute inflammatory response (LAIR pathway). A possible explanation is that immune signals were expressed by tumor cells, thus leading to spillover effect and elevated immune scores in non-proliferative tumor[28].

For survival analysis, it should be noted that both public datasets (METABRIC and SCAN-B) consisted of mostly NSTs. Histology was included in multivariant Cox regression which showed no significance, however, subgroup analysis in NST and ILCs showed change in significance potentially affected by different treatment paradigms of the two datasets (Supplementary Fig. 3). Thus more evidence is needed for applicability of TAM-Low signature as prognostic indicator in ILCs and NSTs respectively.

In conclusion, through integrated RNA-seq and mIHC analysis of ER + /HER2- primary ILC tumors, we found that the proliferative ILC transcriptomic subtype exhibited higher immune infiltration. We would like to propose the TAM-Low signature as a potential novel biomarker for predicting reduced infiltration of pro-inflammatory and pro-tumorigenic macrophages and improved survival in ER+ breast cancer, and encourage its further analysis in additional studies. Future studies are warranted to quantify TAM subtypes in ILC, as indicators of endocrine treatment response and survival, as well as to improve potential use of immunotherapy.

Methods
Ethical regulations
Patient recruitment was described previously[12]. Ethical regulations of this study were approved by the Institutional Review Board at the University of Pittsburgh under the protocol of PRO17100602 and PRO16060685. All participants had submitted written informed consent prior to sample acquisition.

Study design, sample acquisition, and sample processing
For the 21 cases, formalin-fixed paraffin-embedded (FFPE) blocks of primary ER + /HER2- ILC tumors were acquired from University of Pittsburgh Biospecimen Core, and clinical information was queried from the UPMC Cancer Registry. For each block, three sections (at the top, bottom and middle of the block) were stained with hematoxylin and eosin (H&E) and inspected by pathologist to circle out regions with tumor epithelial cell proportion ≥40%. 5 sections (of 10uM thickness each) were used for RNA extraction and sequencing at these circled regions. And another 3 sections (of 4uM thickness each) were used for multispectral immunophenotyping by mIHC.

RNA sequencing and bioinformatics analysis
Sample RNA was extracted with Qiagen tissue DNA/RNA kit from FFPE sections, assessed with High Sensitivity RNA TapeStation for quality and concentration. Library was prepared with illumina TruSeq RNA Library Preparation Kit, and sequenced with Illumina Nextseq 500 75 bp pair-end in 150 cycles at University of Pittsburgh Health Sciences Sequencing Core. For RNA-seq data, we used FastQC for FASTQ data quality control, trimmomatic for adapter trimming, Hisat2 for alignment to human genome 38 (hg38), and HTSeq for quantification, to generate normalized expression in transcripts per million (TPM). To call CDH1 mutations from RNA-seq data, we used GATK v4 MuTect2 pipeline (broad-institute.org) to call all somatic SNVs and indels from bam files calculated with STAR (v2.7.5a), and selected CDH1 mutations from annotation from ANNOVAR[29]. For ILC subtyping, we first trained a Nearest Centroid classifier in original TCGA ILC samples with RNA expression of the 60-gene signature, using original annotation of the proliferative, reactive-like, and immune-related subtypes[6]. We then applied the trained classifier to RNA-seq data of this study, which generated one subtype for each sample. Both training and testing sets were normalized in $\log_2$TPM and transformed into gene-wise z-score. Finally, we combined the reactive-like and immune-related subgroups as the 'non-proliferative' subtype, due to limited sample numbers of both classes. We used GSVA (v1.48.2, ssGSEA) to calculate signature scores of immune-related and cell-cycle related pathways from TPM of our samples. We calculated PAM50 subtype probability with Genefu (v2.26.0), and estimated tumor purity, stromal score, and immune scores using deconvolute_estimate (immunedeconv v2.1.0).

mIHC staining, quantification, and statistical analysis

Workflow of mIHC was described with processed data (median infiltration of each immune cell type at patient level) previously[12]. In brief, FFPE sections of 4 μM thickness were stained with an immunophenotyping panel (CD20, CD4, CD8, FOXP3, CD68, Pan-CK), from which immune cells were counted using InForm software from randomly selected regions of interests (ROI) (3–13/section) at representative immune infiltration areas, from Vectra Polaris (PerkinElmer) scans at ×10. Specifically, infiltration of each immune cell type was calculated in tumor and stromal regions respectively (number/mm^2). We computed Spearman's correlation for abundance of each pair of immune cell types (number/mm^2) and used FDR < 0.05 to select statistically significant correlations. Non-negative matrix factorization was used to cluster ROIs based on Spearman's correlation matrix of log$_2$ normalized counts (BigNmf, v1.0.0). from which 5 clusters were selected based on elbow point of cophenetic correlation coefficient. The corresponding consensus matrix was plotted in Euclidean distance in Ward's linkage.

TAM-Low signature generation and pathway analysis

We calculated Spearman's correlation between expression of each gene (TPM) and abundance of each immune cell type (number/mm^2) at tumor and stromal region (median values among ROIs). A gene-immune cell pair correlation is significant if with FDR < 0.05. Genes which were significantly negatively correlated with stromal or tumor macrophage infiltration were included into 'TAM-Low' signature (483 genes, Fig. 3, Supplementary Fig. 2). Pathway analysis was performed with EnrichR, using Gene Ontology, Kyoto Encyclopedia of Genes and Genomes (KEGG), and Reactome datasets[30].

Public datasets and analysis

Signatures of TAM subtypes were downloaded[18]. We used consensus TME algorithm (immunedeconv v2.1.0, deconvolute_consensus_tme_custom)[28,31] to calculate deconvolution score for TAM-Low and TAM subtype signatures from normalized expression of samples in METABRIC (normalized expression, downloaded from cBioportal)[17], SCAN-B (log$_2$ counts per million)[16], and POETIC trial[32]. Spearman's correlation was calculated between signature scores of every pair of TAM subtypes among samples with FDR correction. In survival analysis, we classified samples by 'TAM-Low' signature expression (high vs low) using optimal cut point (survminer v0.4.9), and calculated hazard ratio from multivariate Cox regression, adjusting for histology, HER2, PR, age at diagnosis, tumor size, and tumor stage (METABRIC[17] and SCAN-B[16]). For POETIC trial data, RNA-seq and responder information were downloaded from GSE105777 and GSE126870[19].

Data availability

RNA-seq data was submitted to SRA database under BioProject:PRJNA1105553, and Gene Expression Omnibus under GSE278301. mIHC ROI quantification data is in Supplementary Table 4.

Code availability

Codes for data analysis and plotting of this manuscript are available on https://github.com/leeoesterreich/ILC-Immune-Infiltration.

References

1. Cortes, J. et al. Pembrolizumab plus chemotherapy in advanced triple-negative breast cancer. *N. Engl. J. Med.* **387**, 217–226 (2022).
2. Schmid, P. et al. Pembrolizumab for early triple-negative breast cancer. *N. Engl. J. Med.* **382**, 810–821 (2020).
3. Cardoso, F. et al. KEYNOTE-756: Randomized, double-blind, phase 3 study of pembrolizumab vs placebo combined with neoadjuvant chemotherapy and adjuvant endocrine therapy for high-risk, early-stage estrogen receptor–positive, human epidermal growth factor receptor 2–negative (ER+/HER2−) breast cancer. American Society of Clinical Oncology; 2019).
4. Loi, S. et al. A phase III trial of nivolumab with neoadjuvant chemotherapy and adjuvant endocrine therapy in ER+/HER2-primary breast cancer: CheckMate 7FL. American Society of Clinical Oncology; 2020).
5. Perou, C. M. et al. Molecular portraits of human breast tumours. *Nature* **406**, 747–752 (2000).
6. Ciriello, G. et al. Comprehensive molecular portraits of invasive lobular breast cancer. *Cell* **163**, 506–519 (2015).
7. Michaut, M. et al. Integration of genomic, transcriptomic and proteomic data identifies two biologically distinct subtypes of invasive lobular breast cancer. *Sci. Rep.* **6**, 1–13 (2016).
8. Jin, X. et al. Molecular classification of hormone receptor-positive HER2-negative breast cancer. *Nat. Genet.* **55**, 1696–1708 (2023).
9. Heindl, A. et al. Relevance of spatial heterogeneity of immune infiltration for predicting risk of recurrence after endocrine therapy of ER+ breast cancer. *JNCI: J. Natl Cancer Inst.* **110**, 166–175 (2018).
10. Aran, D., Hu, Z. & Butte, A. J. xCell: digitally portraying the tissue cellular heterogeneity landscape. *Genome Biol.* **18**, 1–14 (2017).
11. Oshi, M. et al. M1 Macrophage and M1/M2 ratio defined by transcriptomic signatures resemble only part of their conventional clinical characteristics in breast cancer. *Sci. Rep.* **10**, 16554 (2020).
12. Onkar, S. et al. Immune landscape in invasive ductal and lobular breast cancer reveals a divergent macrophage-driven microenvironment. *Nat. Cancer* **4**, 516–534 (2023).
13. Du, T. et al. Invasive lobular and ductal breast carcinoma differ in immune response, protein translation efficiency and metabolism. *Sci. Rep.* **8**, 1–11 (2018).
14. Desmedt, C. et al. Immune infiltration in invasive lobular breast cancer. *J. Natl. Cancer Inst.* **110**, 768–776 (2018).
15. Salgado, R. et al. The evaluation of tumor-infiltrating lymphocytes (TILs) in breast cancer: recommendations by an International TILs Working Group 2014. *Ann. Oncol.* **26**, 259–271 (2015).
16. Saal, L. H. et al. The Sweden Cancerome Analysis Network-Breast (SCAN-B) Initiative: a large-scale multicenter infrastructure towards implementation of breast cancer genomic analyses in the clinical routine. *Genome Med.* **7**, 1–12 (2015).
17. Curtis, C. et al. The genomic and transcriptomic architecture of 2,000 breast tumours reveals novel subgroups. *Nature* **486**, 346–352 (2012).
18. Ma, R.-Y., Black, A. & Qian, B.-Z. Macrophage diversity in cancer revisited in the era of single-cell omics. *Trends Immunol.* **43**, 546–563 (2022).
19. Gao, Q. et al. Impact of aromatase inhibitor treatment on global gene expression and its association with antiproliferative response in ER+ breast cancer in postmenopausal patients. *Breast Cancer Res.* **22**, 1–20 (2020).
20. Abdou, Y. et al. Immunotherapy in triple negative breast cancer: beyond checkpoint inhibitors. *NPJ Breast Cancer* **8**, 121 (2022).
21. Van Baelen, K. et al. Reporting on invasive lobular breast cancer in clinical trials: a systematic review. *NPJ Breast Cancer* **10**, 23 (2024).
22. Egging, D., van Vlijmen-Willems, I., van Tongeren, T., Schalkwijk, J. & Peeters, A. Wound healing in tenascin-X deficient mice suggests that tenascin-X is involved in matrix maturation rather than matrix deposition. *Connect. Tissue Res.* **48**, 93–98 (2007).
23. Yeow, Y. L. et al. Immune-mediated ECM depletion improves tumour perfusion and payload delivery. *EMBO Mol. Med.* **11**, e10923 (2019).
24. Yang, X., Lin, J., Wang, G. & Xu, D. Targeting proliferating tumor-infiltrating macrophages facilitates spatial redistribution of CD8+ T cells in pancreatic cancer. *Cancers* **14**, 1474 (2022).
25. Ramos, R. N. et al. Tissue-resident FOLR2+ macrophages associate with CD8+ T cell infiltration in human breast cancer. *Cell* **185**, 1189–207.e25 (2022).

26. Molgora, M. et al. TREM2 modulation remodels the tumor myeloid landscape enhancing anti-PD-1 immunotherapy. *Cell* **182**, 886–900. e17 (2020).
27. Yofe, I. et al. Spatial and temporal mapping of breast cancer lung metastases identify TREM2 macrophages as regulators of the metastatic boundary. *Cancer Discov.* **13**, 2610–2631 (2023).
28. Sturm, G. et al. Comprehensive evaluation of transcriptome-based cell-type quantification methods for immuno-oncology. *Bioinformatics* **35**, i436–i445 (2019).
29. Wang, K., Li, M. & Hakonarson, H. ANNOVAR: functional annotation of genetic variants from high-throughput sequencing data. *Nucleic Acids Res.* **38**, e164–e164 (2010).
30. Kuleshov, M. V. et al. Enrichr: a comprehensive gene set enrichment analysis web server 2016 update. *Nucleic Acids Res.* **44**, W90–W97 (2016).
31. Jiménez-Sánchez, A., Cast, O. & Miller, M. L. Comprehensive benchmarking and integration of tumor microenvironment cell estimation methods. *Cancer Res.* **79**, 6238–6246 (2019).
32. Anders, S., Pyl, P. T. & Huber, W. HTSeq—a Python framework to work with high-throughput sequencing data. *Bioinformatics* **31**, 166–169 (2015).

Author contributions
S.Oe. and S.On. developed concept and design of this study. S.On., Y.L., and P.L. accomplished data acquisition and pre-processing. F.C. performed formal data analysis, data interpretation, statistical analysis, and drafted the manuscript. J.Z. and Y.L. provided administrative, technical, or material support in data analysis. G.T., T.B., D.A.A.V., S.Oe., and A.V.L. provided supervision. All authors contributed to critical revision of the manuscript for important intellectual content.

Competing interests
D.A.A.V.: cofounder and stock holder—Novasenta, Potenza, Tizona, Trishula; stock holder—Werewolf; patents licensed and royalties—B.M.S., Novasenta; scientific advisory board member—Werewolf, F-Star, Apeximmune, T7/Imreg Bio; consultant—B.M.S., Regeneron, Ono Pharma, Avidity Partners, Peptone; funding—B.M.S., Novasenta. Other authors declare no competing interests.

Additional information
Supplementary information The online version contains supplementary material available at https://doi.org/10.1038/s41698-024-00746-z.

Correspondence and requests for materials should be addressed to Adrian V. Lee or Steffi Oesterreich.

Reprints and permissions information is available at http://www.nature.com/reprints

Publisher's note Springer Nature remains neutral with regard to jurisdictional claims in published maps and institutional affiliations.